

## Chapter 8

# <sup>19</sup>F NMR Probing the Acidity of Frozen Electrolyte Solutions

C. Robinson, C. S. Boxe, M. I. Guzmán, A. J. Colussi,\* and M. R. Hoffmann

W. M. Keck Laboratories, California Institute of Technology, Pasadena, CA 91125

### Abstract

The marginal but selective encapsulation of ions by growing ice induces transient polarizations. Electroneutrality is ultimately restored via  $H^+/OH^-$  interfacial migration producing fluid phases of altered acidity. The media in which solutes become confined upon freezing are, therefore, not only more concentrated but have different acidities than the precursor solutions. This largely unrecognized phenomenon should affect reaction rates and equilibria in frozen aqueous systems. We report, for the first time, measurements of the acidity of extensively frozen dilute solutions of various electrolytes based on the temperature dependence of the <sup>19</sup>F chemical shifts of the 3-fluorobenzoic acid *in situ* probe. We find that acidity significantly increases or decreases upon freezing depending on the type of ions involved. In particular, NaCl, NaNO<sub>2</sub> and KNO<sub>3</sub> solutions become more basic, while NH<sub>4</sub>OH or Na<sub>2</sub>SO<sub>4</sub> solutions become more acidic, upon freezing. The environmental implications of these results are briefly analyzed.

*This chapter has been submitted for publication to Journal of Physical Chemistry (2005).*

## Introduction

The onset of snow photochemistry strongly perturbs the composition of the boundary layer at high latitudes in early spring.<sup>1,2</sup> Nitrogen oxides and, particularly, nitrous acid escape from the snowpack during the solar photolysis of the nitrate ion contaminant.<sup>3-6</sup> These rapid losses are accompanied by a dark process that depletes nitrate for years after deposition.<sup>7,8</sup> The smaller chloride deficits in ice cores dating from the last glacial maximum have been ascribed to the neutralization of normally acidic ice by enhanced dust levels.<sup>9</sup> The pH of seawater has been observed to decrease upon freezing, leading to carbonate precipitation and carbon dioxide degassing.<sup>10</sup> The pH of high alpine lakes was found to be directly correlated with ambient temperature.<sup>11</sup> The tantalizing possibility that such apparently dissimilar phenomena could have a common mechanism remains to be elucidated. A recent analysis of air-snow interactions and their effect on atmospheric chemistry revealed that the role of ionic species in the structure, composition and chemistry of ice/electrolyte interfaces remains poorly understood.<sup>2</sup>

The ubiquitous ice/water interface occurs in important chemical, biological, environmental, and atmospheric processes.<sup>12,13</sup> The existence of a fluid interfacial layer at the air/pristine ice boundary (the “quasi-liquid layer (QLL)”) is just an example of the general phenomenon known as surface melting.<sup>14,15</sup> When dealing with natural systems, it is more relevant, however, to consider the domain of fluidity of partially frozen dilute electrolyte solutions, as well as the composition of the ice (the solidus) and the remaining liquid (the liquidus) in the range of environmentally accessible temperatures.<sup>16,17</sup>

Snow and ice contain solutes of atmospheric or marine origin that are largely segregated into microscopic fluid films because, with few exceptions, ice is notoriously

### VIII-3

intolerant to impurities.<sup>18-22</sup> Hence, during freezing, although most ions largely (> 99.9 %) remain in solution, some are selectively included as substitutional dopants into the growing ice phase depending on the rate of freezing.<sup>23,24</sup> Thus, a transient freezing electric potential develops (superimposed to the intrinsic equilibrium potential of the ice-air interface)<sup>24-28</sup> that can induce thermodynamically favorable,<sup>29-33</sup> as well as unfavorable reactions.<sup>25,34,35</sup>

Freezing will halt when the fluid reaches the composition of the liquidus at the imposed temperature. The residual charge imbalance ultimately relaxes via  $H^+$  and  $OH^-$  (the natural charge carriers of dielectric ice) migration across the ice/solution boundary. If anions (rather than cations) were preferentially rejected from ice during freezing,  $H^+_{aq}$  ( $OH^-_{aq}$ ) will penetrate into the solid to reestablish electroneutrality in all phases. As a result, the liquidus will become less (more) acidic than the initially unfrozen solution.<sup>36,37</sup> The relative affinity of the different ions for ice can be inferred in principle from the sign of the freezing potential of the corresponding solutions.<sup>23</sup> Ion uptake by ice growing from solutions of mixed electrolytes of diverse concentrations, such as those encountered in natural systems, remains a largely unexplored subject. Ammonium ions, for example, are known to enhance incorporation of a variety of anions into the ice matrix.<sup>20</sup>

Except for an isolated study,<sup>37</sup> which employed a pH electrode to monitor the acidity of the (initially 0.1 M neutral) NaCl solution ahead of an ice front, advancing at  $\sim 3 \mu\text{m}$ , Bronshteyn and Chernov's predictions have been directly tested.<sup>36</sup> Specifically, we investigate  $^{19}\text{F}$  chemical shifts (or the relative pH changes) detected by a molecular *in situ* probe, 3-fluorobenzoic acid, embedded in the microscopic fluid films created by the

## VIII-4

extensive freezing of dilute solutions of electrolyte mixtures of environmental relevance over a wide range of freezing conditions.

### Experimental Methods

Single electrolyte solutions of 5 mM and 1 M KNO<sub>3</sub>, NaNO<sub>2</sub>, NaCl, Na<sub>2</sub>SO<sub>4</sub>, and NH<sub>4</sub>OH at 3 < pH < 6 were doped with an *in situ* probe, 10 mM 3-fluorobenzoic acid. A specified volume (90  $\mu$ l) of each solution was transferred by a 100  $\mu$ l Gilson micropipette to a 4 mm diameter zirconia (ZrO<sub>2</sub> with MgO) rotor. Solutions were then sealed inside the rotor by a Kel-F cap.

NMR experiments were performed on a Bruker Avance 500 MHz spectrometer at a 5 kHz spin rate, associated with a superconducting coil, giving a magnetic field of 11.70 T (working frequency for <sup>19</sup>F is 470.70 MHz). Using Bruker Avance 500 MHz spectrometer's respective temperature controller, temperatures were adjusted between 200 and 298 K. A Bruker MAS probe tuned for fluorine (<sup>19</sup>F) was utilized on the rotor. All experiments conducted were single pulsed, where the  $\pi/2$  pulse width was 4  $\mu$ s. <sup>19</sup>F chemical shifts were externally referenced with perfluorooctane (C<sub>8</sub>F<sub>18</sub>) in chloroform (CHCl<sub>3</sub>). Spectra were registered consistently with 16 scans over  $\sim$  90 sec. time periods. Solutions were cooled at 0.5, 1, 2, and 10  $^{\circ}$ C min<sup>-1</sup> and were only heated at 1  $^{\circ}$ C min<sup>-1</sup>. Note: the cooling rates and the heating rate pertain to the rates of cooling and heating between temperatures where spectra were generated.

### Results and Discussion

Nuclear magnetic resonance is the technique of choice used for reporting the molecular environment of solutes in solution.<sup>38</sup> Rotational and translational motions have such different time scales in solids and liquids that it is possible to characterize the pore

## VIII-5

structure of ices by  $^1\text{H}$  NMR imaging.<sup>22,39,40</sup> Chemical shift gradients provide another dimension to the NMR imaging of materials, like their heterogeneity.  $^{19}\text{F}$ -NMR solute probes can transmit acidity changes in aqueous microenvironments based on the  $^{19}\text{F}$  chemical shift differentials between conjugated acids and bases. We chose to monitor acidity changes in extensively frozen solutions by means of 3-fluorobenzoic [ $\text{pK}_a = 3.68$ ,  $\Delta(\delta_{\text{F,acid}} - \delta_{\text{F,anion}} = \text{ppm}]$  as acidity probes.<sup>41</sup> Alternatively, highly sensitive  $^{31}\text{P}$ -NMR pH probes designed for in vivo acidity studies could be used.<sup>42</sup> In general, protonation and dissociation occur so rapidly in the NMR time scales that the measured chemical shift,  $\langle\delta_{\text{F}}\rangle$ , is actually a molar average of anion and undissociated acid contributions:

$$\langle\delta_{\text{F}}\rangle = x\delta_{\text{F,ANION}} + (1-x)\delta_{\text{F,ACID}} \quad (1)$$

i.e.,  $\langle\delta_{\text{F}}\rangle$  is a direct measure of the degree of ionization of  $x$ .

The interpretation of pH measurements at low temperatures requires some precision.<sup>43,44</sup> While the temperature dependence of  $\text{pK}_a$ 's is weak ( $\Delta H_{\text{diss}} \sim 0.5 \text{ kcal mol}^{-1}$ ),<sup>45</sup>  $K_w$  is very sensitive to temperature ( $\Delta H_{\text{diss}} \sim 13.52 \text{ kcal mol}^{-1}$ ).<sup>45</sup> Thus the neutral point of supercooled water at  $-35 \text{ }^\circ\text{C}$  is estimated at pH 8.4. The drastic ionic strength,  $I$ , changes attending massive freezing will significantly affect dissociation equilibria. Therefore, it is problematic to define pH in partially frozen media. However, if one intends to assess the extent of dissociation of a weak acid, e.g., HONO, in frozen electrolyte solutions, most of these effects cancel out. Let us consider how  $\langle\delta_{\text{F}}\rangle$  measurements for a fluoroacid FAH, as a function of temperature, can be used with good approximation to estimate the degree of dissociation of nitrous acid, HONO:

### VIII-6

$$\text{HONO} = \text{NO}_2^- + \text{H}^+ \quad K_N = \frac{[\text{H}^+][\text{NO}_2^-]}{[\text{HONO}]} \times \frac{\gamma_{\text{H}^+} \gamma_{\text{NO}_2^-}}{\gamma_{\text{HONO}}} \quad (2)$$

$$\text{FAH} = \text{FA}^- + \text{H}^+ \quad K_P = \frac{[\text{H}^+][\text{FA}^-]}{[\text{FAH}]} \times \frac{\gamma_{\text{H}^+} \gamma_{\text{FA}^-}}{\gamma_{\text{FAH}}} \quad (3)$$

$$\langle \delta_F \rangle = \delta_{\text{FAH}} + x_{\text{FA}^-} (\delta_{\text{FA}^-} - \delta_{\text{FAH}}) \quad (4)$$

$$x_{\text{FA}^-} = \frac{[\text{FA}^-]}{[\text{FA}^-] + [\text{FAH}]} \quad (5)$$

$$\frac{[\text{HONO}]}{[\text{NO}_2^-]} = \frac{K_P}{K_N} \times \frac{\gamma_{\text{NO}_2^-} \gamma_{\text{FAH}}}{\gamma_{\text{HONO}} \gamma_{\text{FA}^-}} \times \left[ \frac{\delta_{\text{FA}^-} - \delta_{\text{FAH}}}{\langle \delta_F \rangle - \delta_{\text{FAH}}} \right] \quad (6)$$

The relationship  $[\text{HONO}]/[\text{NO}_2^-]$  vs  $\langle \delta_F \rangle$  (Eq. 6) will be, in general, determined by the initial overall composition of the solution and  $T$ . However, the temperature dependence of the ratio of acidity constants, the first factor in the RHS of Equation 6, will be either negligible or readily estimated from independent information. Furthermore, the second factor in the RHS of Equation 6 will be nearly independent of  $T$  and  $I$  due to a mutual cancellation of effects between the activity coefficients of the corresponding anions and undissociated acids. Considering that the chemical shifts of FAH/FA<sup>-</sup> as well as of the reference standard have very weak temperature dependences ( $< 0.001 \text{ ppm K}^{-1}$ ),<sup>46,47</sup> we infer that Equation 6 establishes the basis for the evaluation of the extent of dissociation of weak acids in the liquids of partially frozen solutions.

The <sup>19</sup>F NMR spectra of 10 mM 3-fluorobenzoic acid in variable concentrations (e.g., 5 mM, .5 M, and 1 M) of single electrolyte solutions in D<sub>2</sub>O (MP = 277 K) were recorded as a function of temperature between 200 and 298 K. Using this technique, we have confirmed that acidities significantly increase or decrease upon freezing depending

## VIII-7

on the type of ions involved. For example, the apparent pH increases, overall, during all cooling rates for NaCl, KNO<sub>3</sub>, and NaNO<sub>2</sub> solutions (Figs. 8.1a-e, 8.2a-e, and 8.3a-e). These pH values were derived from the  $\langle\delta_F\rangle$  vs. pH titration curve for 2-fluoroethanoic at 298 K, assuming negligible ( $T, I$ ) effects. Assuming ideal solution behavior, we estimate (from the fusion enthalpy of D<sub>2</sub>O) that at 270 K  $x_{D_2O} = 0.934$ , where  $[NaCl] \sim 3.9$  M (i.e.,  $\sim 98.7\%$  of the solvent has frozen). Figures 8.1b, 8.1d, 8.2b, 8.2d, 8.3b, and 8.3d all reveal the extent of supercooling required to freeze the solutions in a few minutes. It is known that increasing the solute concentration in an ice matrix will enhance surface and interfacial aqueous/ice premelting.<sup>48,49</sup> These figures also show explicitly that solute effects lower the freezing point of the entire ice matrix to a certain temperature, which appears to be electrolyte-specific.

In contrast to the increase in pH during the freezing of NaCl, KNO<sub>3</sub>, and NaNO<sub>2</sub> solutions, Na<sub>2</sub>SO<sub>4</sub> and NH<sub>4</sub>OH solutions display the opposite effect (Fig. 8.4a-c and 8.5a-d). While the plotted pH values should be corrected to take into account these effects (see above), the opposite acidity trends displayed by NaCl and Na<sub>2</sub>SO<sub>4</sub> solutions upon freezing seem well established by these preliminary experiments. Freezing hysteresis loops are also shown in Figures 8.4a, 8.4c, and 8.5a. Similarly, Figures 8.4 and 8.5 display freezing point depression, such as the 203 K freezing point of 1 M NH<sub>4</sub>OH (Fig. 8.5d). Since chemical shifts of the partially frozen solutions remain constant for about 60 minutes after ice separation has taken place, they are ascribed to thermally and chemically equilibrated systems.

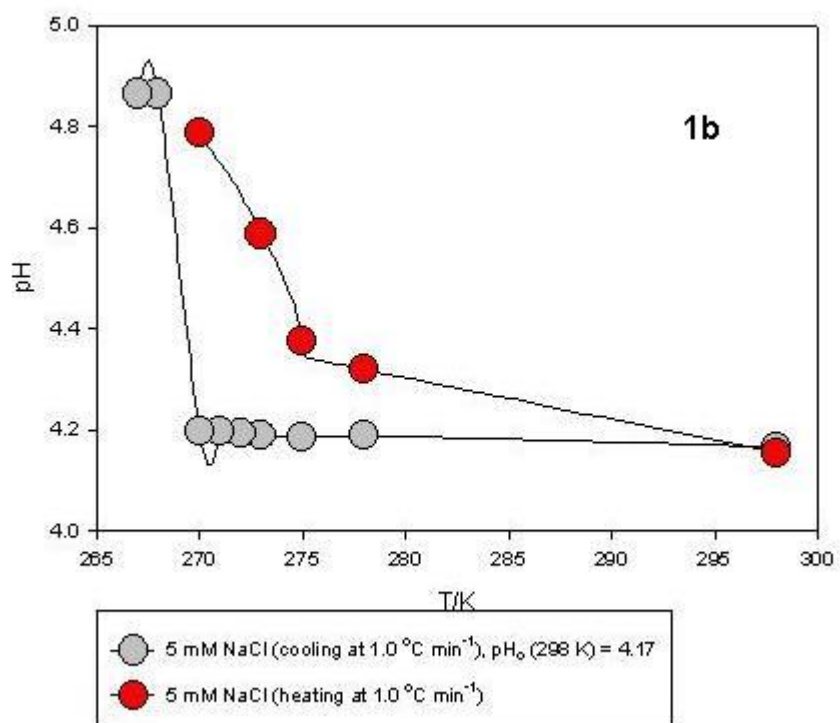
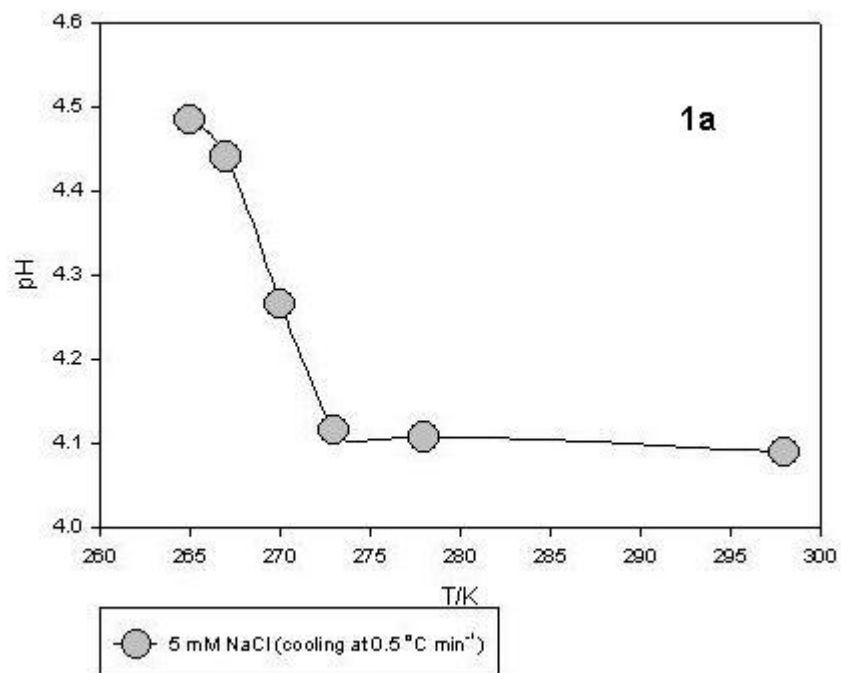
It is apparent that by measuring the average chemical shifts of adequate pH probes as function of temperature in solutions duplicating the overall ionic composition

## VIII-8

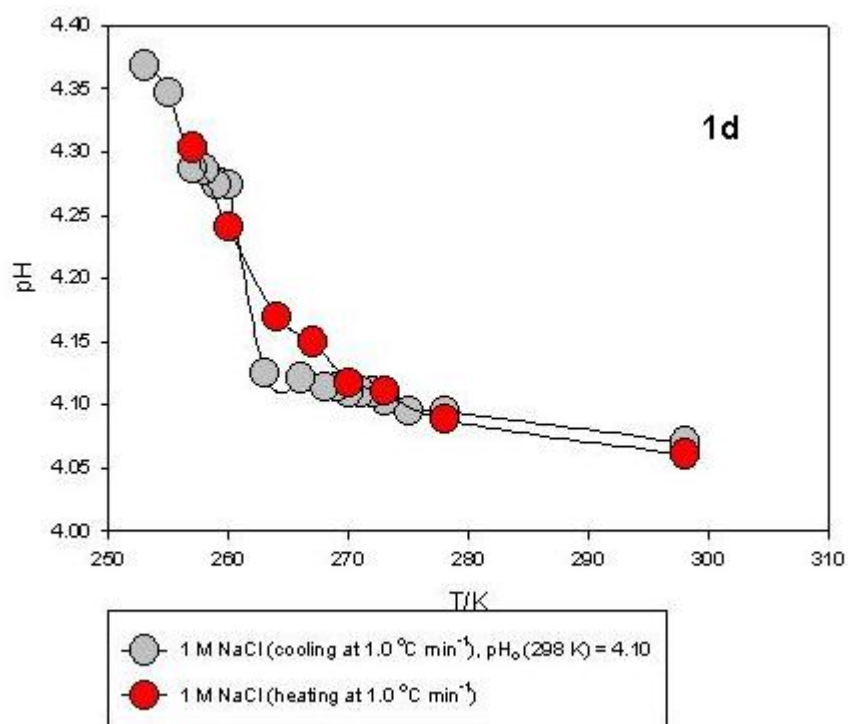
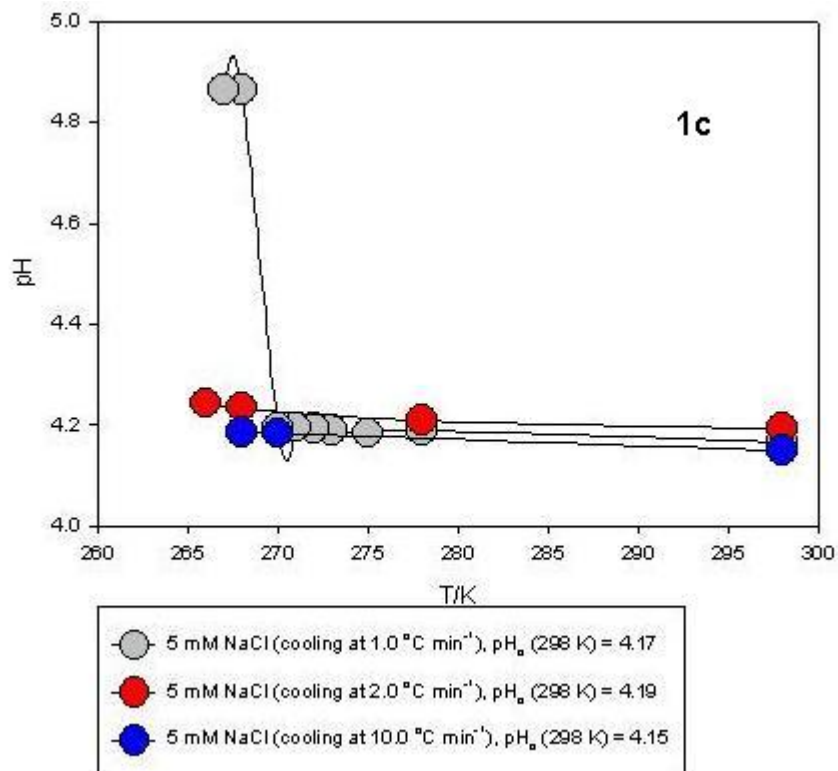
of ambient snow, it should be feasible to evaluate the acidity of the solutes milieu under all conditions. These phenomena are directly relevant to polar environments, where in acidic snow-covered regions, nitrite ( $pK_a \sim 3.2$ ) will protonate to form nitrous acid, which will in turn, be released readily as  $\text{HONO}_{(g)}$  from the snowpack.<sup>3,5,50,51</sup> Zhou *et al.*<sup>3</sup> measured excessive levels of  $\text{HONO}_{(g)}$  at Alert, Canada, where the freezing mechanism, causing a reduction in acidity of the ice medium, will be directly relevant.



### VIII-9



## VIII-10



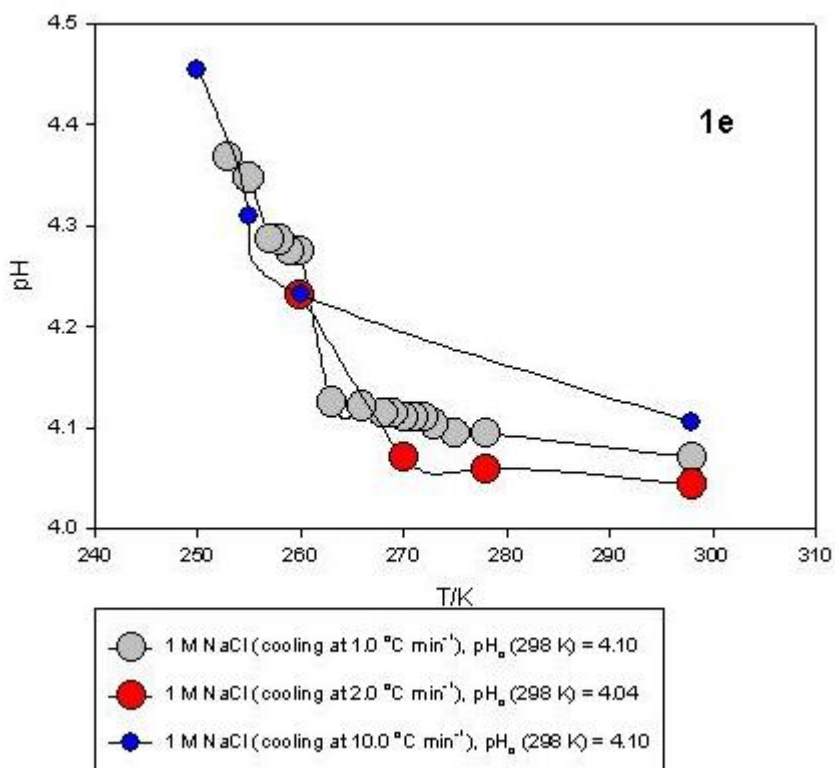
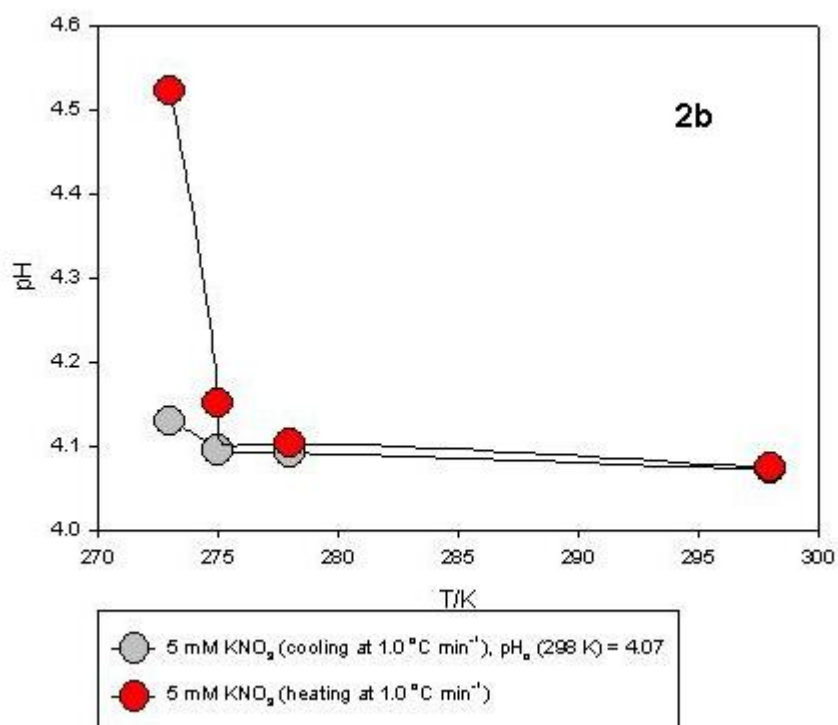
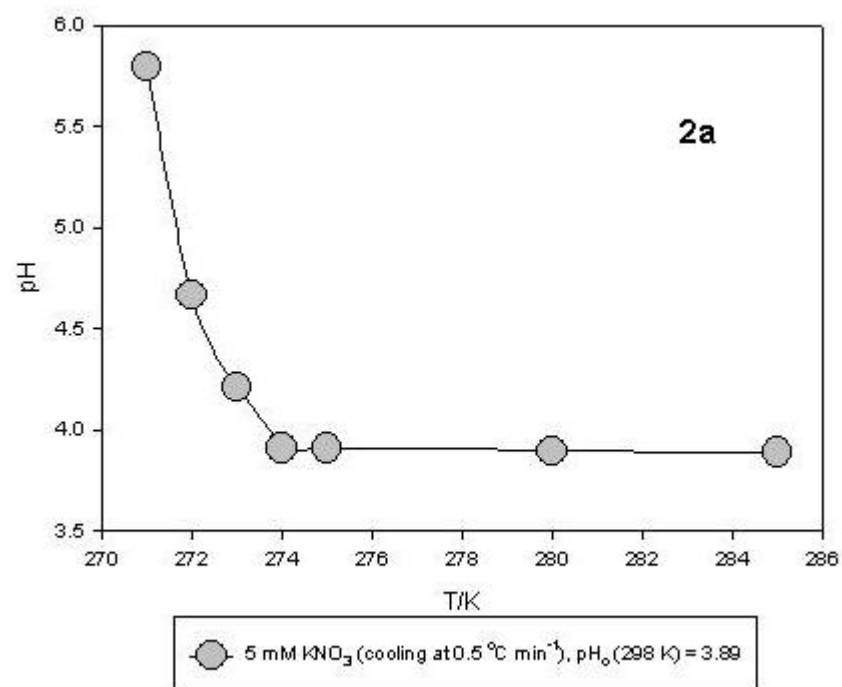
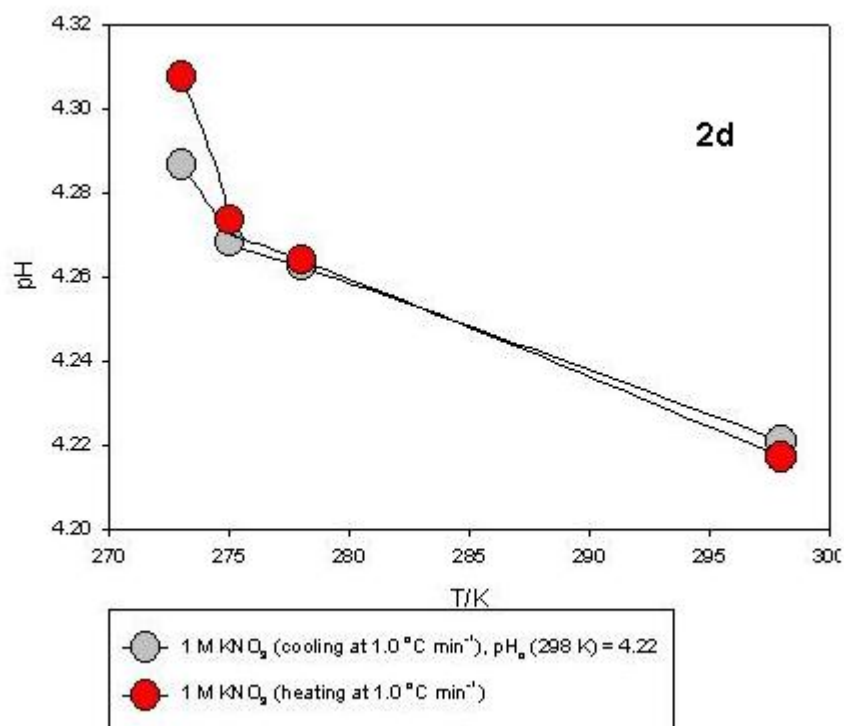
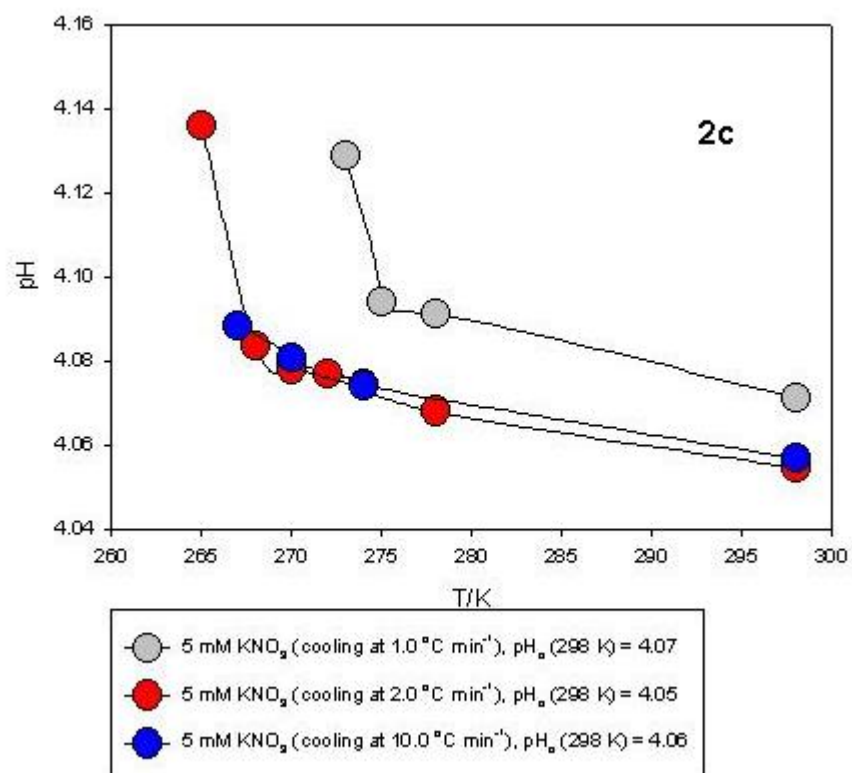


**Figure 8.1.** 1a: (●) 5 mM NaCl cooling at 0.5 °C min<sup>-1</sup> from 298 to 265 K. 1b: (●) 5 mM NaCl cooling at 1.0 °C min<sup>-1</sup> from 298 to 267 K; (●) 5 mM NaCl heating at 1.0 °C min<sup>-1</sup> from 267 to 298 K. 1c: (●) 5 mM NaCl cooling at 1.0 °C min<sup>-1</sup> from 298 to 267 K; (●) 5 mM NaCl cooling at 2.0 °C min<sup>-1</sup> from 298 to 266 K; (●) 5 mM NaCl cooling at 10.0 °C min<sup>-1</sup> from 298 to 268 K. 1d: (●) 1 M NaCl cooling at 1.0 °C min<sup>-1</sup> from 298 to 253 K; (●) 1 M NaCl heating at 1.0 °C min<sup>-1</sup> from 253 to 298 K. 1e: (●) 1 M NaCl cooling at 1.0 °C min<sup>-1</sup> from 298 to 253 K; (●) 1 M NaCl cooling at 2.0 °C min<sup>-1</sup> from 298 to 260 K; (●) 1 M NaCl cooling at 10.0 °C min<sup>-1</sup> from 298 to 250 K.

## VIII-12



## VIII-13



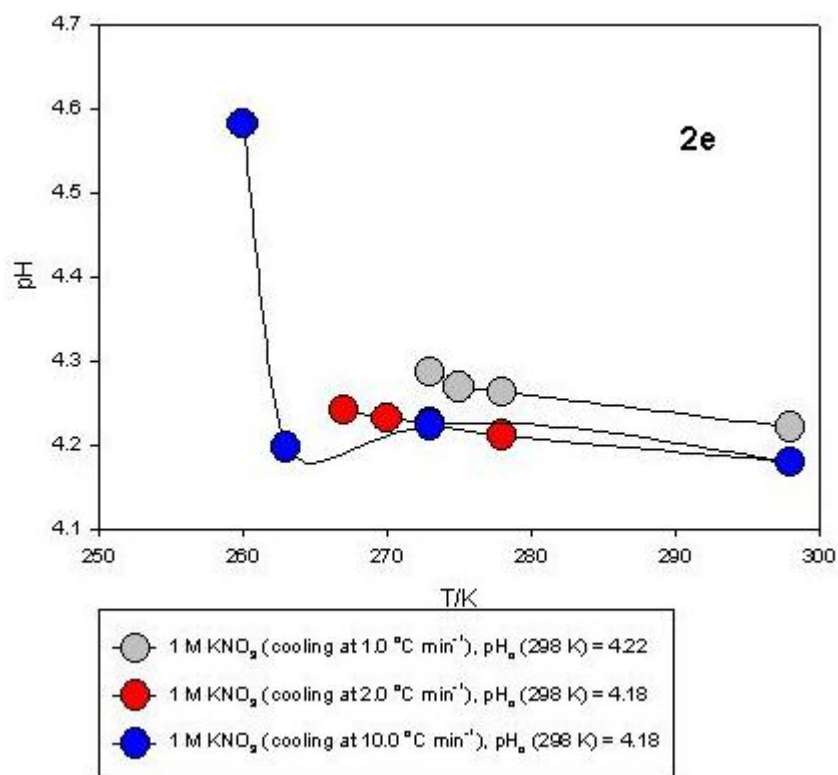
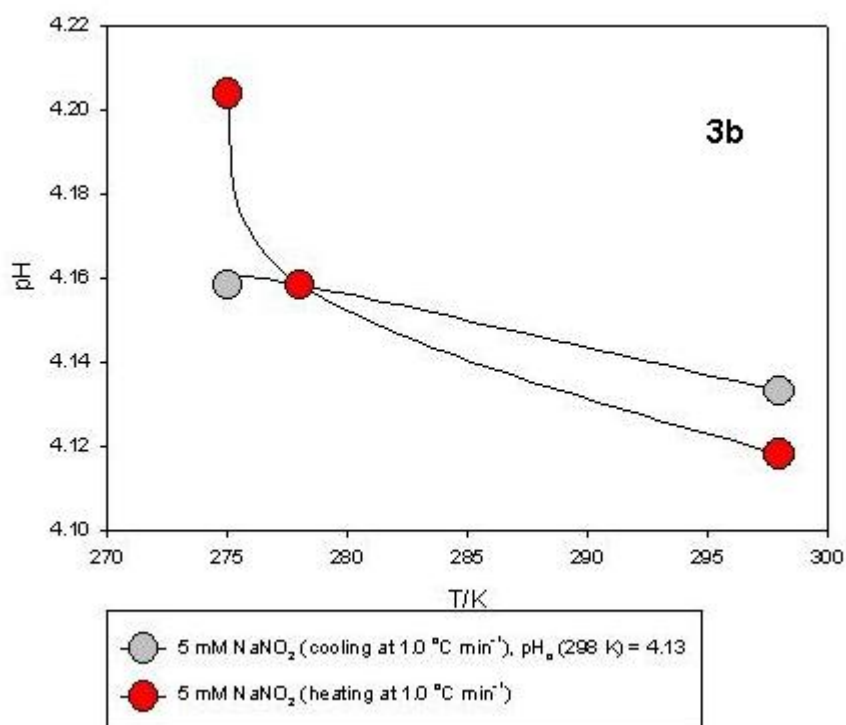
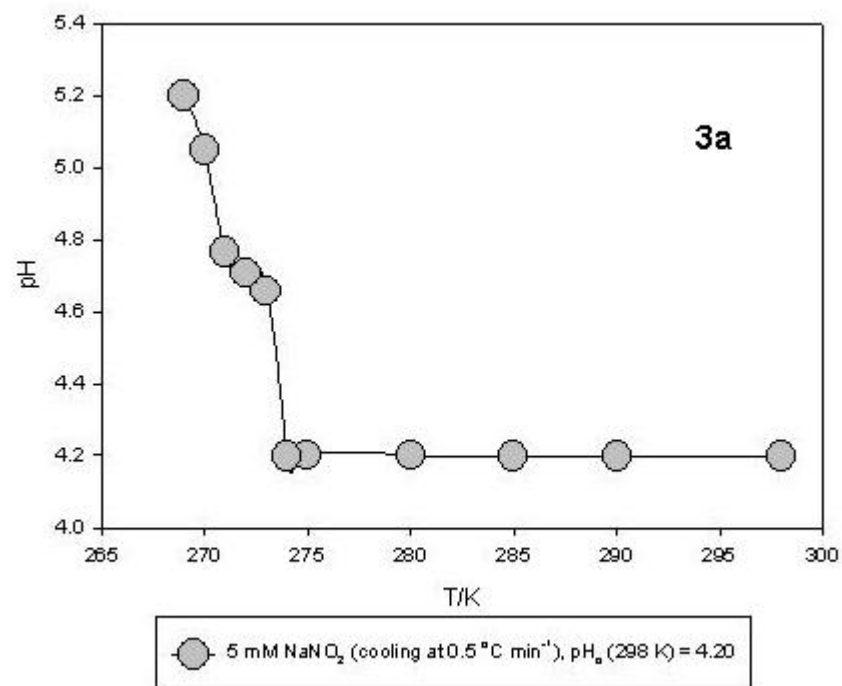
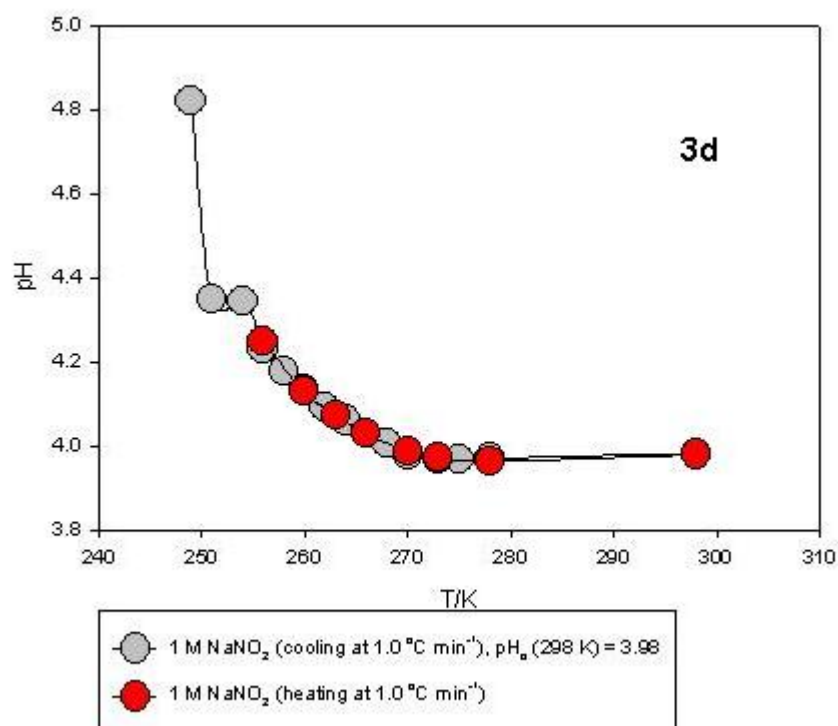
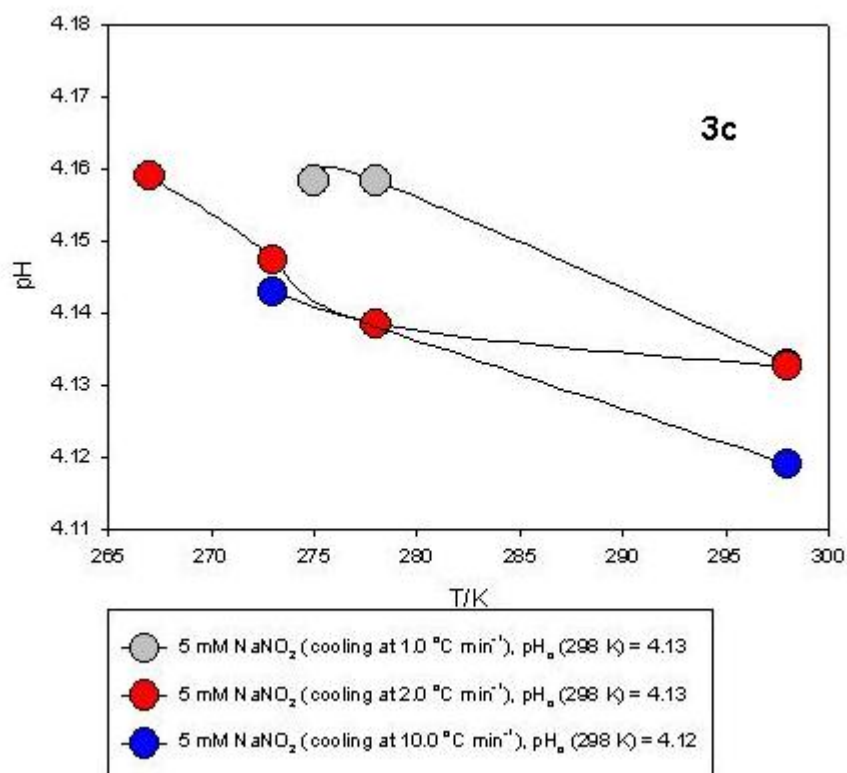


**Figure 8.2.** 2a: (●) 5 mM KNO<sub>3</sub> cooling at 0.5 °C min<sup>-1</sup> from 298 to 271 K. 2b: (●) 5 mM KNO<sub>3</sub> cooling at 1.0 °C min<sup>-1</sup> from 298 to 273 K; (●) 5 mM KNO<sub>3</sub> heating at 1.0 °C min<sup>-1</sup> from 273 to 298 K. 2c: (●) 5 mM KNO<sub>3</sub> cooling at 1.0 °C min<sup>-1</sup> from 298 to 273 K; (●) 5 mM KNO<sub>3</sub> cooling at 2.0 °C min<sup>-1</sup> from 298 to 265 K; (●) 5 mM KNO<sub>3</sub> cooling at 10.0 °C min<sup>-1</sup> from 298 to 267 K. 2d: (●) 1 M KNO<sub>3</sub> cooling at 1.0 °C min<sup>-1</sup> from 298 to 273 K; (●) 1 M KNO<sub>3</sub> heating at 1.0 °C min<sup>-1</sup> from 273 to 298 K. 2e: (●) 1 M KNO<sub>3</sub> cooling at 1.0 °C min<sup>-1</sup> from 298 to 273 K; (●) 1 M KNO<sub>3</sub> cooling at 2.0 °C min<sup>-1</sup> from 298 to 267 K; (●) 1 M KNO<sub>3</sub> cooling at 10.0 °C min<sup>-1</sup> from 298 to 260 K.

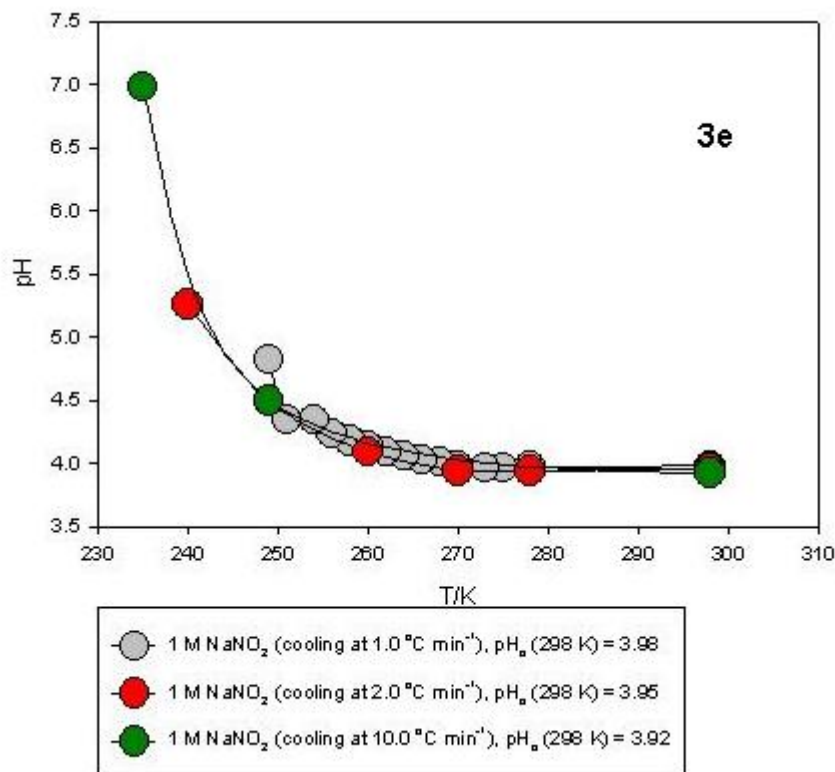
## VIII-15



## VIII-16

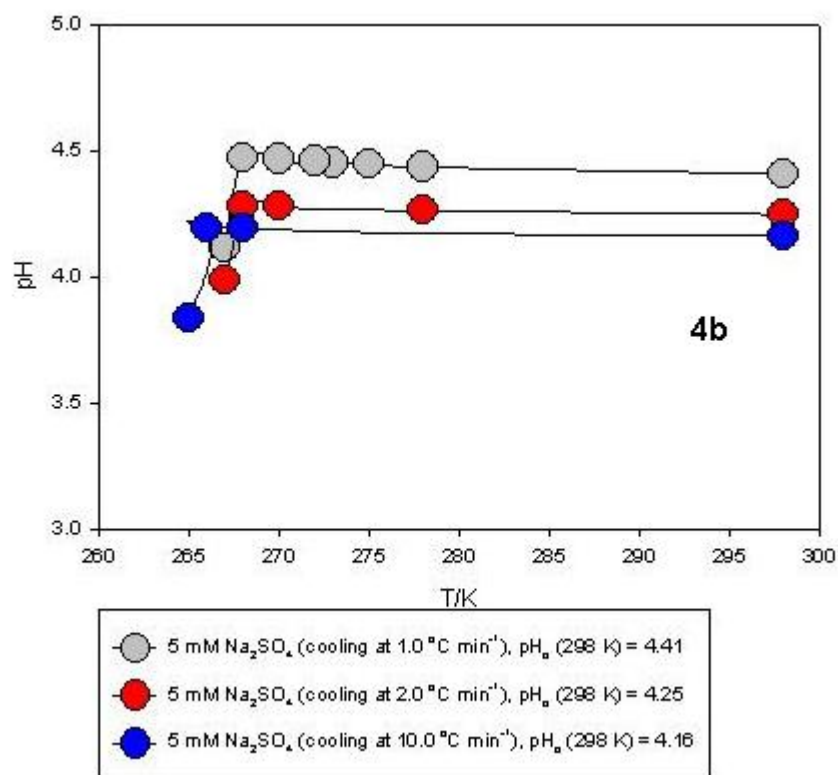
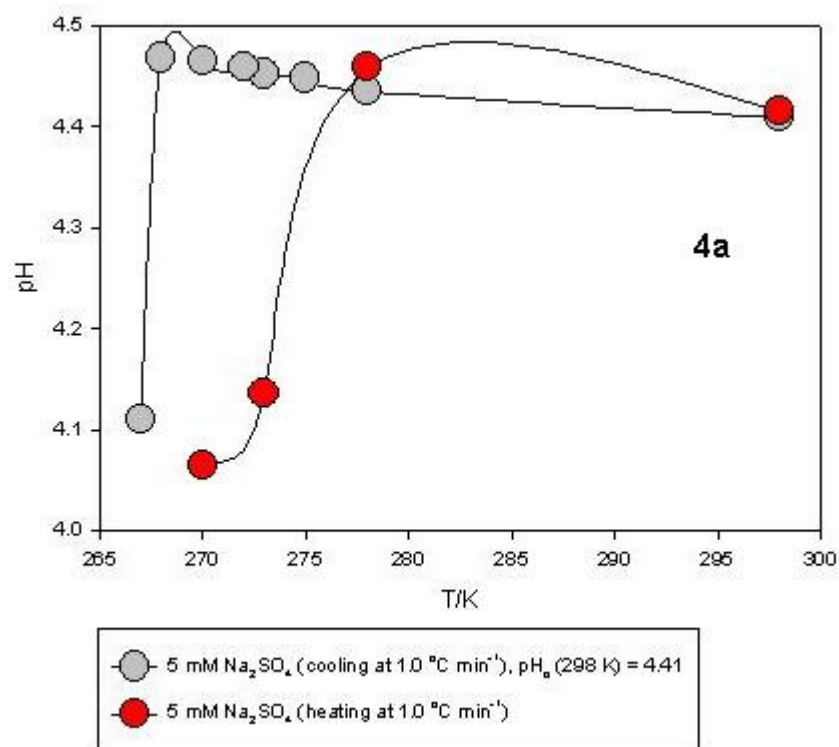






**Figure 8.3.** 3a: (●) 5 mM NaNO<sub>2</sub> cooling at 0.5 °C min<sup>-1</sup> from 298 to 269 K. 3b: (●) 5 mM NaNO<sub>2</sub> cooling at 1.0 °C min<sup>-1</sup> from 298 to 275 K; (●) 5 mM KNO<sub>3</sub> heating at 1.0 °C min<sup>-1</sup> from 275 to 298 K. 3c: (●) 5 mM KNO<sub>3</sub> cooling at 1.0 °C min<sup>-1</sup> from 298 to 275 K; (●) 5 mM KNO<sub>3</sub> cooling at 2.0 °C min<sup>-1</sup> from 298 to 267 K; (●) 5 mM KNO<sub>3</sub> cooling at 10.0 °C min<sup>-1</sup> from 298 to 263 K. 3d: (●) 1 M KNO<sub>3</sub> cooling at 1.0 °C min<sup>-1</sup> from 298 to 249 K; (●) 1 M KNO<sub>3</sub> heating at 1.0 °C min<sup>-1</sup> from 249 to 298 K. 3e: (●) 1 M KNO<sub>3</sub> cooling at 1.0 °C min<sup>-1</sup> from 298 to 249 K; (●) 1 M KNO<sub>3</sub> cooling at 2.0 °C min<sup>-1</sup> from 298 to 240 K; (●) 1 M KNO<sub>3</sub> cooling at 10.0 °C min<sup>-1</sup> from 298 to 235 K.

## VIII-18



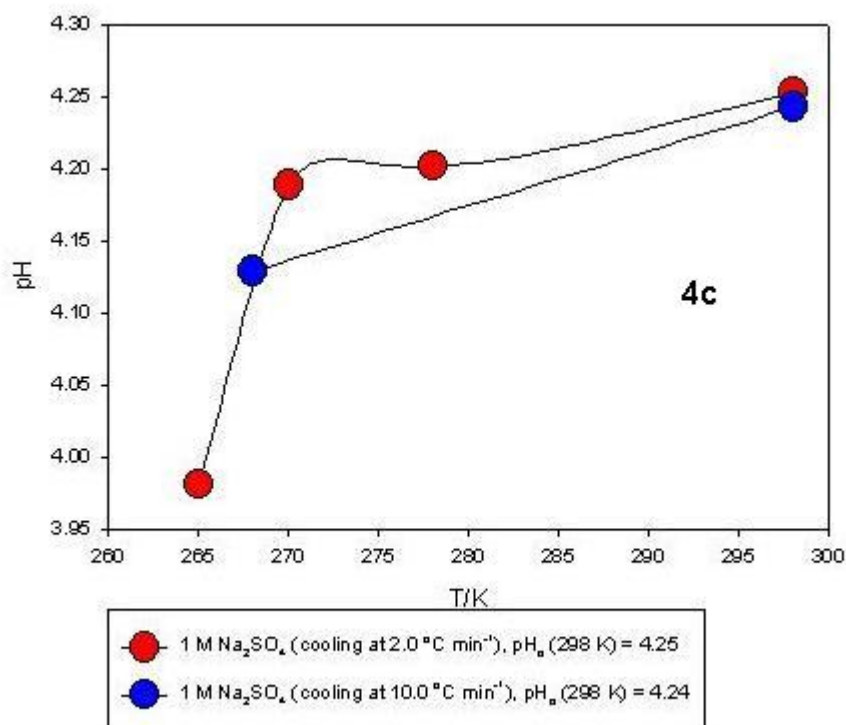
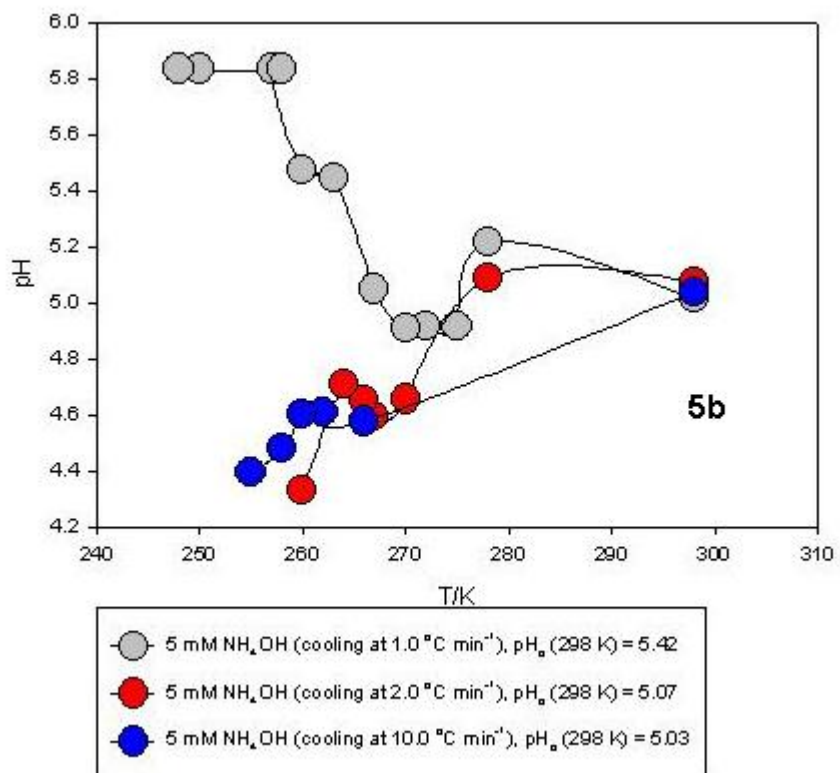
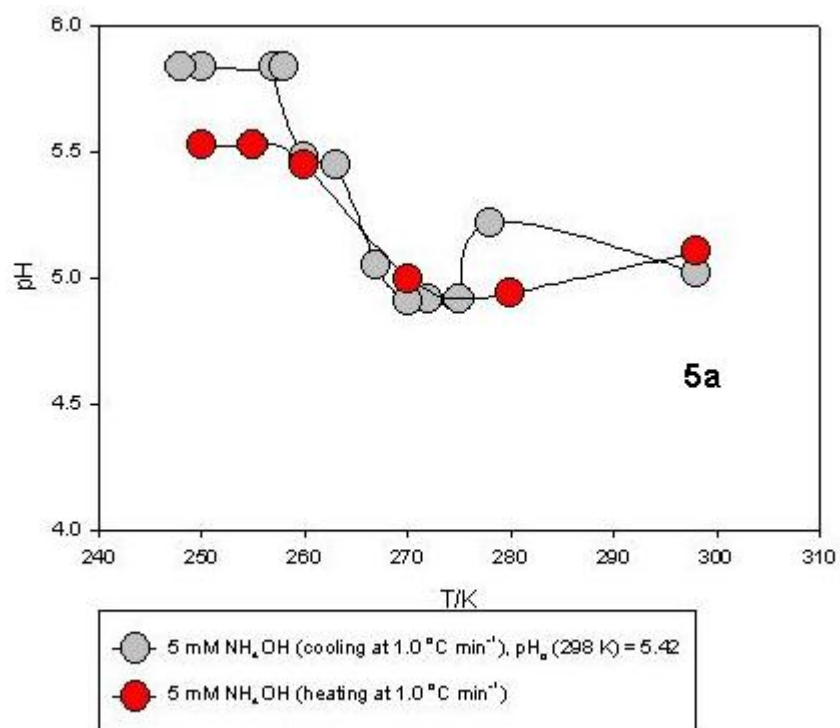
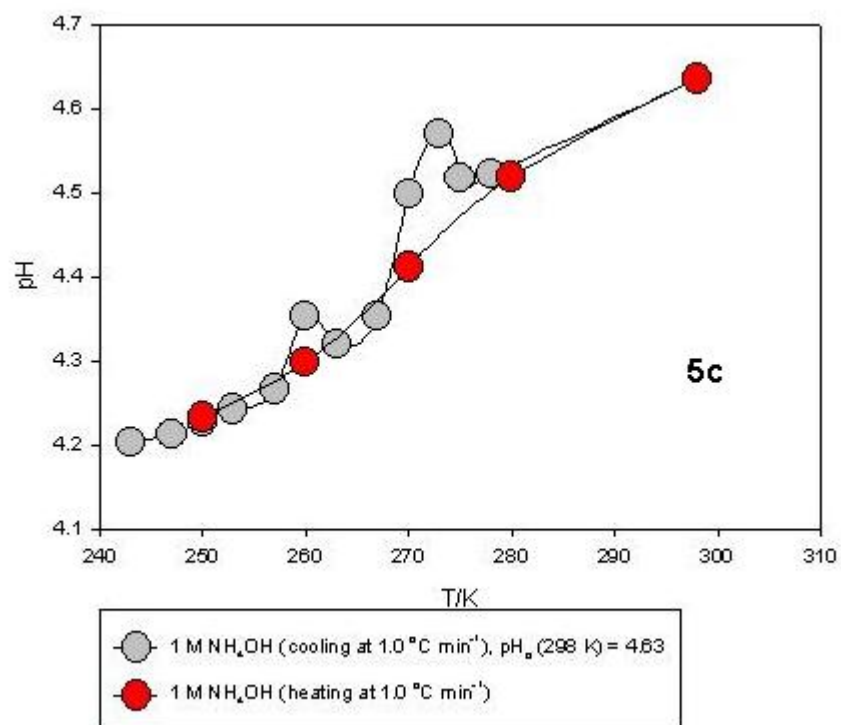


**Figure 8.4.** 4a: (●) 5 mM Na<sub>2</sub>SO<sub>4</sub> cooling at 1.0 °C min<sup>-1</sup> from 298 to 267 K; (●) 5 mM Na<sub>2</sub>SO<sub>4</sub> heating at 1.0 °C min<sup>-1</sup> from 267 to 298 K. 4b: (●) 5 mM Na<sub>2</sub>SO<sub>4</sub> cooling at 1.0 °C min<sup>-1</sup> from 298 to 267 K; (●) 5 mM Na<sub>2</sub>SO<sub>4</sub> cooling at 2.0 °C min<sup>-1</sup> from 298 to 267 K; (●) 5 mM Na<sub>2</sub>SO<sub>4</sub> cooling at 10.0 °C min<sup>-1</sup> from 298 to 265 K. 4c: (●) 1 M Na<sub>2</sub>SO<sub>4</sub> cooling at 2.0 °C min<sup>-1</sup> from 298 to 268 K; (●) 1 M Na<sub>2</sub>SO<sub>4</sub> cooling at 10.0 °C min<sup>-1</sup> from 298 to 268 K.

## VIII-20



# VIII-21



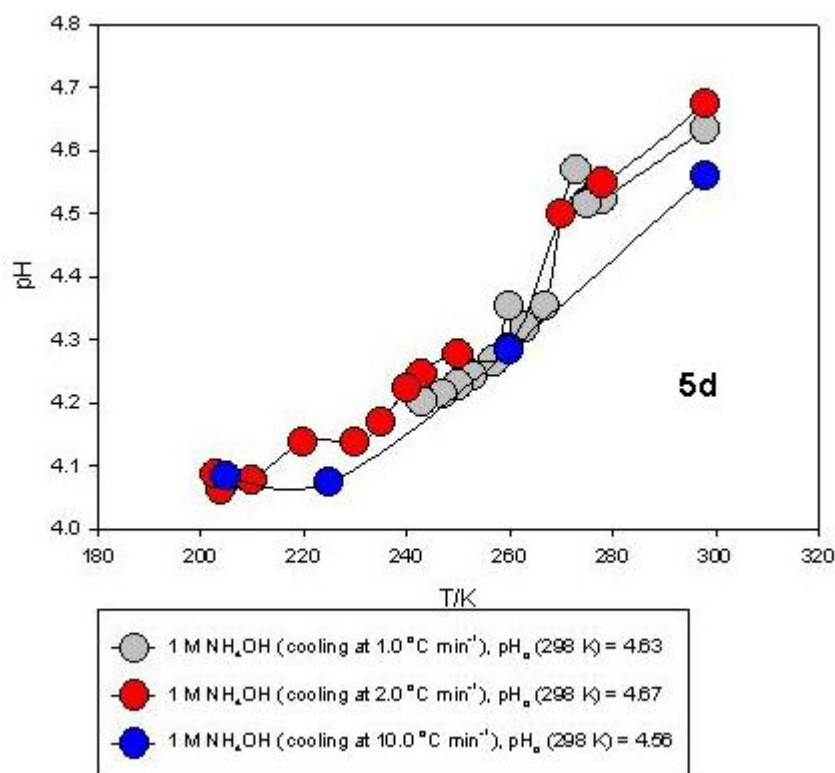


**Figure 8.5.** 1a: (●) 5 mM NH<sub>4</sub>OH cooling at 1.0 °C min<sup>-1</sup> from 298 to 248 K; (●) 5 mM NH<sub>4</sub>OH heating at 1.0 °C min<sup>-1</sup> from 248 to 298 K. 1b: (●) 5 mM NH<sub>4</sub>OH cooling at 1.0 °C min<sup>-1</sup> from 298 to 248 K; (●) 5 mM NH<sub>4</sub>OH cooling at 2.0 °C min<sup>-1</sup> from 298 to 260 K; (●) 5 mM NH<sub>4</sub>OH cooling at 10.0 °C min<sup>-1</sup> from 298 to 255 K. 1c: (●) 1 M NH<sub>4</sub>OH cooling at 1.0 °C min<sup>-1</sup> from 298 to 243 K; (●) 1 M NH<sub>4</sub>OH heating at 1.0 °C min<sup>-1</sup> from 243 to 298 K. 1d: (●) 1 M NH<sub>4</sub>OH cooling at 1.0 °C min<sup>-1</sup> from 298 to 243 K; (●) 1 M NH<sub>4</sub>OH cooling at 2.0 °C min<sup>-1</sup> from 298 to 203 K; (●) 1 M NH<sub>4</sub>OH cooling at 10.0 °C min<sup>-1</sup> from 298 to 205 K.

## References

- (1) Albert, M. R.; Grannas, A. M.; Bottenheim, J.; Shepson, P. B.; Perron, F. E. *Atmos. Environ.* **2002**, *36*, 2779.
- (2) Domine, F.; Shepson, P. B. *Science* **2002**, *297*, 1506.
- (3) Zhou, X. L.; Beine, H. J.; Honrath, R. E.; Fuentes, J. D.; Simpson, W.; Shepson, P. B.; Bottenheim, J. W. *Geophysical Research Letters* **2001**, *28*, 4087.
- (4) Honrath, R. E.; Guo, S.; Peterson, M. C.; Dziobak, M. P.; Dibb, J. E.; Arsenault, M. A. *J. Geophys. Res.-Atmos.* **2000**, *105*, 24183.
- (5) Dibb, J. E.; Arsenault, M.; Peterson, M. C.; Honrath, R. E. *Atmos. Environ.* **2002**, *36*, 2501.
- (6) Anastasio, C.; Jordan, A. L. *Atmos. Environ.* **2004**, *38*, 1153.
- (7) Mulvaney, R.; Wagenbach, D.; Wolff, E. W. *J. Geophys. Res.* **1998**, *103*, 11021.
- (8) Rothlisberger, R.; Hutterli, M. A.; Wolff, E. W.; Mulvaney, R.; Fischer, H.; Bigler, M.; Goto-Azuma, K.; Hansson, M. E.; Ruth, U.; Siggaard-Andersen, M. L.; Steffensen, J. P. Nitrate in Greenland and Antarctic ice cores: a detailed description of post-depositional processes. In *Annals Of Glaciology, Vol 35*; Int Glaciological Soc: Cambridge, **2002**; Vol. 35; pp 209.
- (9) Rothlisberger, R.; Mulvaney, R.; Wolff, E. W.; Hutterli, M. A.; Bigler, M.; de Angelis, M.; Hansson, M. E.; Steffensen, J. P.; Udisti, R. *J. Geophys. Res.-Atmos.* **2003**, *108*.
- (10) Papadimitriou, S.; Kennedy, H.; Kattner, G.; Dieckmann, G. S.; Thomas, D. N. *Geochim. Cosmochim. Acta* **2004**, *68*, 1749.

- 11) Koinig, K. A.; Schmidt, R.; Sommaruga-Wograth, S.; Tessadri, R.; Psenner, R.  
*Water Air Soil Pollut.* **1998**, *104*, 167.
- 12) Petrenko, V. F.; Whitworth, R. W. *Physics of Ice*; University Press: Oxford, 1999.
- 13) Bryk, T.; Haymet, A. D. J. *J. Mol. Liq.* **2004**, *112*, 47.
- 14) Ewing, G. E. *J. Phys. Chem. B* **2004**, *108*, 15953.
- 15) Henson, B. F.; Robinson, J. M. *Phys. Rev. Lett.* **2004**, *92*.
- 16) Reisman, A. *Phase Equilibria*; Academic: New York, 1970.
- 17) Tsionsky, V.; Zagidulin, D.; Gileadi, E. *J. Phys. Chem. B* **2002**, *106*, 13089.
- 18) Gross, G. W.; McKee, C.; Wu, C. H. *J. Chem. Phys.* **1975**, *62*, 3080.
- 19) Gross, G. W.; Gutjahr, A.; Caylor, K. *J. Physique* **1987**, *48*, 527.
- 20) Gross, G. W.; Svec, R. K. *J. Phys. Chem. B* **1997**, *101*, 6282.
- 21) Killawee, J. A.; Fairchild, I. J.; Tison, J. L.; Janssens, L.; Lorrain, R. *Geochim. Cosmochim. Acta* **1998**, *62*, 3637.
- 22) Menzel, M. I.; Han, S. I.; Stapf, S.; Blumich, B. *J. Magn. Reson.* **2000**, *143*, 376.
- 23) Workman, E. J.; Reynolds, S. E. *Phys. Rev.* **1950**, *78*, 254.
- 24) Dash, J. G.; Wettlaufer, J. S. *Can. J. Phys.* **2003**, *81*, 201.
- 25) Finnegan, W. G.; Pitter, R. L. *Atmos. Environ. A-Gen.* **1991**, *25*, 2912.
- 26) Kallay, N.; Cakara, D. *J. Colloid Interface Sci.* **2000**, *232*, 81.
- 27) Shibkov, A. A.; Golovin, Y. I.; Zheltov, M. A.; Korolev, A. A.; Leonov, A. A. *J. Cryst. Growth* **2002**, *236*, 434.
- 28) Kallay, N.; Cop, A.; Chibowski, E.; Holysz, L. *J. Colloid Interface Sci.* **2003**, *259*, 89.
- 29) Pincock, R. E. *Accounts Chem. Res.* **1969**, *2*, 97.



- (30) Takenaka, N.; Ueda, A.; Maeda, Y. *Nature* **1992**, 358, 736.
- (31) Takenaka, N.; Ueda, A.; Daimon, T.; Bandow, H.; Dohmaru, T.; Maeda, Y. *J. Phys. Chem.* **1996**, 100, 13874.
- (32) Takenaka, N.; Daimon, T.; Ueda, A.; Sato, K.; Kitano, M.; Bandow, H.; Maeda, Y. *J. Atmos. Chem.* **1998**, 29, 135.
- (33) Betterton, E. A.; Anderson, D. J. *J. Atmos. Chem.* **2001**, 40, 171.
- (34) Finnegan, W. G.; Pitter, R. L.; Young, L. G. *Atmos. Environ. A-Gen.* **1991**, 25, 2531.
- (35) Finnegan, W. G.; Pitter, R. L.; Hinsvark, B. A. *J. Colloid Interface Sci.* **2001**, 242, 373.
- (36) Bronshteyn, V. L.; Chernov, A. A. *J. Cryst. Growth* **1991**, 112, 129.
- (37) Sola, M. I.; Corti, H. R. *An. Asoc. Quim. Argent.* **1993**, 81, 483.
- (38) Cho, H.; Shepson, P. B.; Barrie, L. A.; Cowin, J. P.; Zaveri, R. *J. Phys. Chem. B* **2002**, 106, 11226.
- (39) Blumich, B. *NMR Imaging of Materials*; Clarendon Press: Oxford, **2000**.
- (40) Duer, M. J. *Solid-State NMR Spectroscopy*; Blackwell: Oxford, 2004.
- (41) Boiadjev, S. E.; Lightner, D. A. *J. Phys. Org. Chem.* **1999**, 12, 751.
- (42) Martel, S.; Clement, J. L.; Muller, A.; Culcasi, M.; Pietri, S. *Bioorg. Med. Chem.* **2002**, 10, 1451.
- (43) Bates, R. G. *Determination of pH*; Wiley: New York, 1964.
- (44) Taylor, M. J. *Cryo-Lett.* **1981**, 2, 231.
- (45) Kortum, B. *Treatise on Electrochemistry*; Elsevier: Amsterdam, 1965.
- (46) Jameson, A. K.; Jameson, C. J. *J. Am. Chem. Soc.* **1973**, 95, 8559.

- (47) Llor, J.; Munoz, L. *J. Org. Chem.* **2000**, *65*, 2716.
- (48) Wettlaufer, J. S. *Phys. Rev. Lett.* **1999**, *82*, 2516.
- (49) Doppenschmidt, A.; Butt, H. J. *Langmuir* **2000**, *16*, 6709.
- (50) Li, S.-M. *Atmos. Environ.* **1993**, *27A*, 2959.
- (51) Li, S.-M. *J. Geophys. Res.* **1994**, *99*, 25469.